

Improved GPR-Based CSI Acquisition via Spatial-Correlation Kernel

Syed Luqman Shah[✉], *Graduate Student Member, IEEE*, Nurul Huda Mahmood[✉], *Member, IEEE*, and Italo Atzeni[✉], *Senior Member, IEEE*

Abstract—Accurate channel estimation with low pilot overhead and computational complexity is key to efficiently utilizing multi-antenna wireless systems. Motivated by the evolution from purely statistical descriptions toward physics- and geometry-aware propagation models, this work focuses on incorporating channel information into a Gaussian process regression (GPR) framework for improving the channel estimation accuracy. In this work, we propose a GPR-based channel estimation framework along with a novel *Spatial-correlation* (SC) kernel that explicitly captures the channel’s second-order statistics. We derive a closed-form expression of the proposed SC-based GPR estimator and prove that its posterior mean is optimal in terms of minimum mean-square error (MMSE) under the same second-order statistics, without requiring the underlying channel distribution to be Gaussian. Our analysis reveals that, with up to 50% pilot overhead reduction, the proposed method achieves the lowest normalized mean-square error, the highest empirical 95% credible-interval coverage, and superior preservation of spectral efficiency compared to benchmark estimators, while maintaining lower computational complexity than the conventional MMSE estimator.

Index Terms—6G, Gaussian process regression, MIMO channel estimation, pilot reduction, *Spatial-correlation*.

I. INTRODUCTION

GAUSSIAN process regression (GPR) has emerged as a promising approach for channel state information (CSI) acquisition under tight pilot budgets [1], [2], which is critical for 6G-and-beyond wireless networks [3]. In contrast, conventional least-squares (LS) and minimum mean-square error (MMSE) estimators require pilot sequences whose length scales with the number of transmit antennas, resulting in substantial overhead for large antenna arrays [4]. Though techniques based on compressed sensing mitigate this overhead by exploiting sparsity in the angular or delay domains [4], [5], their performance is sensitive to noise and violations of low-rank assumptions in rich-scattering environments [6]. These limitations motivate the use of GPR-based CSI acquisition, which offers improved estimation accuracy [1] while reducing the pilot overhead [2], [4].

GPR provides a non-parametric Bayesian framework for channel estimation, encoding prior knowledge through a covariance function (kernel). The posterior mean yields the channel estimate, while the posterior covariance quantifies its uncertainty [4], [7]. GPR-based models have been successfully applied to interference prediction and proactive resource allocation [8], hardware distortion modeling [9], and CSI prediction for future channel forecasting [10]. More recently, [2], [4]

The authors are with Centre for Wireless Communications, University of Oulu, Finland (e-mail: {syed.luqman, nurulhuda.mahmood, italo.atzeni}@oulu.fi). This work was supported by the Research Council of Finland (336449 Profi6, 348396 HIGH-6G, 359850 6G-ConCoRSe, and 369116 6G Flagship). Reproducible codes for this work are available at: <https://github.com/Syed-Luqman-Shah-19/MIMOGPR2>.

modeled wireless propagation over a two-dimensional antenna grid and showed that observing only a subset of transmit antennas channel response enables reconstruction of unobserved channel entries. Despite these advances, existing GPR-based channel estimation methods [1], [2], [4] suffer from three fundamental limitations: i) marginal-likelihood-based hyperparameter learning incurs rapidly increasing computational complexity with antenna dimension [7]; ii) commonly used distance-based covariance kernels implicitly assume stationarity and weak anisotropy, leading to model mismatch in channels with direction-dependent scattering and non-separable transmit-receive coupling [11]; and iii) prior second-order channel statistics are not explicitly incorporated under sparse training, limiting systematic exploitation of known covariance structures [2].

This work builds on the reduced-pilot GPR framework proposed in [2] and addresses the above limitations by introducing a novel *Spatial-correlation* (SC) kernel that is induced directly by the channel covariance. Unlike distance-based kernels, the proposed SC kernel derives its covariance from established channel models. This eliminates marginal-likelihood hyperparameter learning and reduces computational complexity while improving estimation accuracy under sparse training. We show that the proposed SC kernel is positive semidefinite (PSD). Based on the SC kernel, we propose an SC-based GPR estimator (SC-GPR). We derive a closed-form expression for the proposed SC-GPR estimator whose posterior mean is MMSE-optimal under the same second-order statistics. The resulting SC-GPR further exploits the structure of standard channel models to enable scalable implementation. In addition to achieving the MMSE mean, the proposed SC-GPR offers the following advantages: i) reduced pilot overhead; ii) uncertainty-aware channel estimates via credible intervals; and iii) lower computational cost. We validate the proposed approach using two closed-form channel covariance families under three reduced-overhead schemes that decrease the pilot load by 50%, 67%, and 75%, respectively. Numerical results show that, even with a 50% pilot reduction, the proposed method achieves lower normalized mean-square error (NMSE) than the benchmark schemes. With a 75% reduction, it further outperforms the benchmarks in terms of spectral efficiency (SE), while also incurring lower computational complexity than the optimal MMSE estimator.

II. SYSTEM MODEL

We consider a narrowband point-to-point MIMO link with N_t transmit antennas and N_r receive antennas. During the channel estimation phase, the pilot overhead is reduced by activating only a subset of the N_t antennas instead of sounding the entire array. Specifically, only $n_t < N_t$ transmit antennas

are activated, which relaxes the requirement on the pilot length from $T \geq N_t$ to $T \geq n_t$ [2]. The pilots transmitted by these n_t active antennas are received across all the N_r receive antennas [4]. Let $\Omega_t = \{a_1, \dots, a_{n_t}\} \subset \{1, \dots, N_t\}$ denote an ordered index set corresponding to the n_t antennas, with no repeated elements. We adopt a structured equispaced activation pattern with stride $\Delta \in \mathbb{N}$, with $a_i = 1 + (i-1)\Delta$ for $i = 1, \dots, n_t$, where $n_t = \lfloor (N_t-1)/\Delta \rfloor + 1$ is the maximum integer satisfying the array-size constraint $1 + (n_t-1)\Delta \leq N_t$.

Let $\mathbf{S} \in \mathbb{C}^{n_t \times T}$ denote the pilot matrix transmitted by the n_t transmit antennas, whose rows are orthonormal and satisfy $\mathbf{S}\mathbf{S}^H = \mathbf{I}_{n_t}$. Based on Ω_t , we define the antenna-selection matrix $\mathbf{F} = [\mathbf{e}_{a_1} \dots \mathbf{e}_{a_{n_t}}] = \mathbf{I}_{N_t}(:, \Omega_t) \in \{0, 1\}^{N_t \times n_t}$, with $\mathbf{F}^H \mathbf{F} = \mathbf{I}_{n_t}$ and where \mathbf{e}_{a_i} denotes the a_i -th canonical basis vector. The resulting transmitted pilot signal is $\mathbf{X} = \mathbf{F}\mathbf{S} \in \mathbb{C}^{N_t \times T}$. The received signal is given by $\mathbf{Y} = \mathbf{H}\mathbf{X} + \mathbf{N} = \mathbf{H}\mathbf{F}\mathbf{S} + \mathbf{N}$, where $\mathbf{H} \in \mathbb{C}^{N_r \times N_t}$ denotes the channel matrix and \mathbf{N} is the noise matrix with i.i.d. $\mathcal{CN}(0, \sigma_n^2)$ entries. Despreading the pilots by right-multiplication with \mathbf{S}^H yields the observation matrix $\tilde{\mathbf{Y}} = \mathbf{Y}\mathbf{S}^H = \mathbf{H}\mathbf{F} + \mathbf{N}\mathbf{S}^H \in \mathbb{C}^{N_r \times n_t}$. Thus, $\tilde{\mathbf{Y}}$ contains noisy observations of the n_t sounded columns of \mathbf{H} indexed by Ω_t [4], while the remaining $N_t - n_t$ channel columns remain unobserved and are inferred via the proposed SC-GPR method at the receiver, as detailed in the following section. Equivalently, these matrix observations correspond to noisy samples of individual channel entries indexed on the antenna grid, which we use as training set for GPR.

III. THE PROPOSED GPR WITH THE SC KERNEL

This section introduces the proposed SC-GPR estimator, establishes its statistical properties, and presents a scalable inference routine for reduced-pilot CSI acquisition. Our approach adopts the proposed SC kernel for GPR, which: i) encodes the channel's second-order structure; ii) removes hyperparameter training to reduce the computation cost; iii) yields a closed-form estimator with calibrated uncertainty; and iv) exploits model structure for scalability. The proposed SC kernel prior captures anisotropy and non-separable transmit-receive coupling implied by standard covariance models, which are not represented by conventional distance-based kernels. As a result, the proposed SC-GPR enables more accurate channel reconstruction under sparse sounding.

Training and test sets: Define the antenna index grid $\mathcal{G} = \{(r, t) : r \in \{1, \dots, N_r\}, t \in \{1, \dots, N_t\}\} \subset \mathbb{N}^2$, which serves as the input domain of the GPR. Let the observed (training) index set be $\mathcal{X} = \{(r, a_i) : r = 1, \dots, N_r, i = 1, \dots, n_t\} \subset \mathcal{G}$, with cardinality $|\mathcal{X}| = P = N_r n_t$, while the unobserved (test) set is $\mathcal{X}_* = \mathcal{G} \setminus \mathcal{X}$ with cardinality $|\mathcal{X}_*| = M$. Each observed entry of $\tilde{\mathbf{Y}}$ corresponds to a noisy sample of a channel coefficient, i.e., $\tilde{Y}_{r,i} = H_{r,a_i} + w_{r,i}$ for $i = 1, \dots, n_t$, with $w_{r,i} \sim \mathcal{CN}(0, \sigma_n^2)$. Thus, the training input locations are stacked as $\mathbf{Z} = [\mathbf{z}_1, \dots, \mathbf{z}_P]^\top \in \mathbb{N}^{P \times 2}$, with $\mathbf{z}_n = (r_n, a_{i_n}) \in \mathcal{X}$, and the corresponding complex-valued observations are collected in $\mathbf{h} = [h_1, \dots, h_P]^\top \in \mathbb{C}^P$, with $h_n = \tilde{Y}_{r_n, i_n}$. We denote the GPR training dataset by $\mathcal{D} = (\mathbf{Z}, \mathbf{h})$. Similarly, the test input locations are given by $\mathbf{Z}_* = [\mathbf{z}_{*,1}, \dots, \mathbf{z}_{*,M}]^\top \in \mathbb{N}^{M \times 2}$, with $\mathbf{z}_{*,m} = (r_{*,m}, t_{*,m}) \in \mathcal{X}_*$, and the unknown test outputs are denoted by $\mathbf{h}_* = [h_{*,1}, \dots, h_{*,M}]^\top \in \mathbb{C}^M$, with

$h_{*,m} = H_{r_{*,m}, t_{*,m}}$. We model $\{H_{r,t}\}$ as a zero-mean proper complex GP over \mathcal{G} , with covariance specified by the proposed SC kernel described next.

SC kernel definition: Let $\mathbf{u} = \text{vec}(\mathbf{H}) \in \mathbb{C}^{N_r N_t}$ denote the column-wise vectorization of the channel matrix. We index the channel coefficient $H_{r,t}$ by $n = r + (t-1)N_r$, with $n \in \{1, \dots, N_r N_t\}$ and $\mathbf{u}[n] = H_{r,t}$. Likewise, (r', t') is mapped to $m = r' + (t'-1)N_r$, with $\mathbf{u}[m] = H_{r',t'}$. The channel covariance matrix is defined as $\mathbf{R}_H = \mathbb{E}[\mathbf{u}\mathbf{u}^H] \in \mathbb{C}^{N_r N_t \times N_r N_t}$, whose (n, m) -th entry is given by $\mathbf{R}_H[n, m] = \mathbb{E}[H_{r,t} H_{r',t'}^*] \in \mathbb{C}$. We define the SC kernel as

$$k_{\text{SC}}((r, t), (r', t')) = \mathbf{R}_H[n, m], \quad (1)$$

which yields a Hermitian kernel suitable for proper complex GPR. From $k_{\text{SC}}(\cdot)$, we construct the Gram matrices $\mathbf{K} = k_{\text{SC}}(\mathbf{Z}, \mathbf{Z}) \in \mathbb{C}^{P \times P}$, $\mathbf{K}_* = k_{\text{SC}}(\mathbf{Z}, \mathbf{Z}_*) \in \mathbb{C}^{P \times M}$, and $\mathbf{K}_{**} = k_{\text{SC}}(\mathbf{Z}_*, \mathbf{Z}_*) \in \mathbb{C}^{M \times M}$ [7]. The resulting GPR posterior for the test locations \mathcal{X}_* is

$$\hat{\mathbf{h}}_* = \mathbf{K}_*^H (\mathbf{K} + \sigma_n^2 \mathbf{I}_P)^{-1} \mathbf{h} \in \mathbb{C}^{M \times 1}, \quad (2)$$

where $\mathbf{h} \in \mathbb{C}^{P \times 1}$ contains the complex-valued training observations, $\hat{\mathbf{h}}_* \in \mathbb{C}^{M \times 1}$ stacks the posterior means, and $\Sigma_* = \mathbf{K}_{**} - \mathbf{K}_*^H (\mathbf{K} + \sigma_n^2 \mathbf{I}_P)^{-1} \mathbf{K}_* \in \mathbb{C}^{M \times M}$ is the posterior covariance [7], [8].

Next, Proposition 1 proves that $k_{\text{SC}}(\cdot)$ is a valid kernel, i.e., for any finite index set, its Gram matrix is Hermitian PSD, ensuring well-posed GPR posteriors and numerically stable inference. Moreover, Proposition 2 shows that the SC-GPR posterior mean equals the MMSE estimator induced by the same second-order model, establishing linear-optimality without assuming channel Gaussianity. In the following, we use the notations $\text{Cov}(\mathbf{a}) = \mathbb{E}[\mathbf{a}\mathbf{a}^H]$ and $\text{Cov}(\mathbf{ab}) = \mathbb{E}[\mathbf{ab}^H]$.

Proposition 1 (Positive semidefiniteness of k_{SC}): Let \mathbf{R}_H be Hermitian PSD. For any finite set $\{\mathbf{z}_m\}_{m=1}^M \subset \mathcal{G}$, the Gram matrix with entries $[k_{\text{SC}}(\mathbf{z}_m, \mathbf{z}_{m'})]_{m,m'} \in \mathbb{C}^{M \times M}$ is Hermitian PSD.

Proof: Index $\mathbf{z}_m = (r_m, t_m)$ by $i_m = (t_m-1)N_r + r_m$ and define $\mathbf{E} = [\mathbf{e}_{i_1}, \dots, \mathbf{e}_{i_M}] \in \mathbb{C}^{(N_r N_t) \times M}$. Then, we have $\mathbf{K} = \mathbf{E}^H \mathbf{R}_H \mathbf{E}$, which is Hermitian. Furthermore, for any $\beta \in \mathbb{C}^M$, we have $\beta^H \mathbf{K} \beta = (\mathbf{E}\beta)^H \mathbf{R}_H (\mathbf{E}\beta) \geq 0$, since \mathbf{R}_H is Hermitian PSD. Hence, we obtain $\mathbf{K} \succeq 0$. ■

Proposition 2 (Posterior mean equals MMSE): Let \mathbf{u} be zero-mean with covariance $\mathbf{R}_H \succeq 0$. Define $\mathbf{y} = \mathbf{B}\mathbf{u} + \mathbf{\varepsilon}$, with $\mathbb{E}[\mathbf{\varepsilon}] = \mathbf{0}$ and $\text{Cov}(\mathbf{\varepsilon}) = \sigma_n^2 \mathbf{I}_P$, where $\mathbf{B} \in \{0, 1\}^{P \times N_r N_t}$ selects the P observed entries. Among the linear estimators $\hat{\mathbf{u}} = \mathbf{Ly}$, the MMSE estimator that minimizes $\mathbb{E}\|\mathbf{u} - \hat{\mathbf{u}}\|_2^2$ is

$$\hat{\mathbf{u}} = \mathbf{R}_H \mathbf{B}^H (\mathbf{B} \mathbf{R}_H \mathbf{B}^H + \sigma_n^2 \mathbf{I}_P)^{-1} \mathbf{y}, \quad (3)$$

with error covariance $\mathbf{C} = \mathbf{R}_H - \mathbf{R}_H \mathbf{B}^H (\mathbf{B} \mathbf{R}_H \mathbf{B}^H + \sigma_n^2 \mathbf{I}_P)^{-1} \mathbf{B} \mathbf{R}_H$. A zero-mean GP prior whose kernel induces \mathbf{R}_H (e.g., k_{SC}) yields a posterior mean that matches (3).

Proof: For $\hat{\mathbf{u}} = \mathbf{Ly}$, the mean-square error is given by $\text{tr}(\mathbf{R}_H - 2\mathbf{L}\text{Cov}(\mathbf{y}, \mathbf{u}) + \mathbf{L}\text{Cov}(\mathbf{y})\mathbf{L}^H)$, with $\text{Cov}(\mathbf{y}, \mathbf{u}) = \mathbf{B}\mathbf{R}_H$ and $\text{Cov}(\mathbf{y}) = \mathbf{B}\mathbf{R}_H \mathbf{B}^H + \sigma_n^2 \mathbf{I}_P$. Differentiating w.r.t. \mathbf{L} and setting the gradient to zero gives $\mathbf{L}^* = \mathbf{R}_H \mathbf{B}^H (\mathbf{B} \mathbf{R}_H \mathbf{B}^H + \sigma_n^2 \mathbf{I}_P)^{-1}$, which yields (3). With a GP prior inducing \mathbf{R}_H , the GP posterior mean has the same form, so $k_{\text{SC}}(\cdot)$ coincides with the MMSE. ■

| Estimator | Complexity | Remarks |
|-----------------------------|----------------------------|---------------------------------------------------------------------------------------------------------------------------------------------------|
| SC-GPR (proposed) | $\mathcal{O}(P^3)$ | \mathbf{K} is indexed from \mathbf{R}_H in (1); no hyperparameter loop; one Cholesky solve of $\mathbf{K} + \sigma_n^2 \mathbf{I}_P$. |
| Learning-based GPR [2], [4] | $\mathcal{O}(QP^3)$ | Q marginal-likelihood iterations; each builds the $P \times P$ kernel, factors $\mathbf{K} + \sigma_n^2 \mathbf{I}_P$, and computes gradients. |
| MMSE | $\mathcal{O}((N_t N_t)^3)$ | Solves a system of size $N_t N_t$; no calibrated uncertainty. |
| LS | $\mathcal{O}(N_t N_t T)$ | Point estimates only; lowest cost but noise-limited; no spatial prior or uncertainty. |

TABLE I: Computational complexity comparison.

Comparing (2) with (3) shows that $k_{SC}(\cdot)$ implements the MMSE estimator implied by \mathbf{R}_H and, in addition, provides calibrated per-entry and joint uncertainty via Σ_* .

Complex channel reconstruction: The complex GP posterior in (2) directly provides $\hat{H}_{r,t}$ for each $(r, t) \in \mathcal{X}_*$ together with its posterior uncertainty.

Computational complexity: SC-GPR offers efficiency relative to learning-based GPR [1], [2], [4] and to the LS and MMSE baselines with full-array training. Specifically, since $P = N_t n_t$ is the number of observed channel entries, computing the SC-GPR posterior in (2) requires forming the $P \times P$ Gram matrix and solving a single linear system via Cholesky factorization, resulting in a computational complexity of $\mathcal{O}(P^3)$. This cost arises from the inversion (or factorization) of $\mathbf{K} + \sigma_n^2 \mathbf{I}_P$ and dominates all the other operations. In learning-based GPR [1], [2], [4], the hyperparameters are learned via marginal-likelihood maximization. Each of the Q outer iterations assembles the $P \times P$ kernel matrix, factors $\mathbf{K} + \sigma_n^2 \mathbf{I}_P$, and evaluates the kernel gradients, leading to an overall complexity of $\mathcal{O}(QP^3)$, as summarized in Table I. In contrast, in SC-GPR the kernel $k_{SC}(\cdot)$ is fully determined by the channel covariance \mathbf{R}_H , the Gram matrices are obtained by direct indexing, and no outer optimization loop is required. Compared to the full-array training MMSE estimator, which involves solving a linear system of dimension $N_t N_t$ and thus scales as $\mathcal{O}((N_t N_t)^3)$, SC-GPR achieves a strictly lower computational complexity for $n_t < N_t$. Hence, SC-GPR provides: i) an MMSE-equivalent posterior mean implied by \mathbf{R}_H ; ii) calibrated per-entry uncertainty from the GP posterior; and iii) scalable computation that explicitly exploits the channel structure.

IV. NUMERICAL EVALUATION

We evaluate the proposed SC-GPR framework under reduced-pilot training to quantify its performance. In particular, we consider three pilot subsampling factors, $\Delta \in \{2, 3, 4\}$, corresponding to 50%, 67%, and 75% reduced training overheads, respectively. Unless stated otherwise, the simulation parameters are summarized in Table II.

We compare the proposed SC-GPR method with the learning-based GPR estimators from [2] employing distance-based kernels, namely the radial basis function (RBF), $k_{RBF}(\mathbf{z}, \mathbf{z}_*) = \gamma_{RBF} \exp(-\|\mathbf{z} - \mathbf{z}_*\|^2/(2\ell_{RBF}^2))$, the Matérn, $k_{Mat}(\mathbf{z}, \mathbf{z}_*) = \gamma_{Mat} \frac{2^{1-\nu}}{\Gamma(\nu)} \left(\frac{\sqrt{2\nu}\|\mathbf{z} - \mathbf{z}_*\|}{\ell_{Mat}}\right)^\nu K_\nu\left(\frac{\sqrt{2\nu}\|\mathbf{z} - \mathbf{z}_*\|}{\ell_{Mat}}\right)$, and the rational quadratic (RQ), $k_{RQ}(\mathbf{z}, \mathbf{z}_*) = \gamma_{RQ}(1 + \|\mathbf{z} - \mathbf{z}_*\|^2/(2\ell_{RQ}^2))^{-\alpha}$.

| System Parameter | Symbol | Value |
|-----------------------------------------------|-------------------------------------------|------------------------|
| Array and propagation | | |
| Receive \times transmit antennas | $N_t \times N_t$ | 36×36 |
| Antenna activation stride | Δ | $\{2, 3, 4\}$ |
| Element spacing | | 0.5 |
| Carrier frequency | | 28 GHz |
| Azimuth angle spread | | $\pi/6$ rad |
| Training / SNR model | | |
| Pilot lengths for SC-GPR | $T = n_t$ | $\{18, 12, 9\}$ |
| Pilot length for the baselines | $T = N_t$ | 36 |
| SNR | ρ | $1/\sigma_n^2$ |
| Learning-based GPR hyperparameters [2] | | |
| Kernels scale (init; bounds) | $\gamma_{RBF}, \gamma_{Mat}, \gamma_{RQ}$ | $1.0; [10^{-2}, 10^2]$ |
| RBF lengthscale (init; bounds) | ℓ_{RBF} | $0.5; [10^{-2}, 10]$ |
| Matérn lengthscale (init; bounds) | ℓ_{Mat} | $0.5; [10^{-2}, 10]$ |
| Matérn smoothness | ν | 1.5 (fixed) |
| RQ lengthscale (init; bounds) | ℓ_{RQ} | $0.5; [10^{-2}, 5]$ |
| RQ shape (init; bounds) | α | $0.5; [10^{-1}, 5]$ |

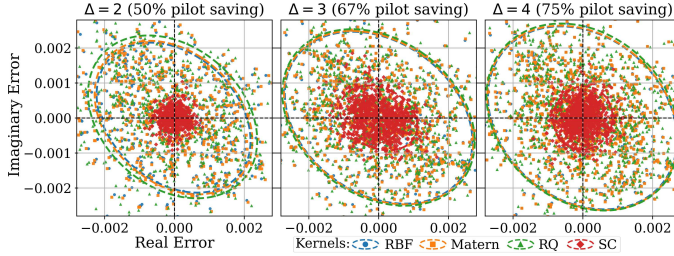
TABLE II: Simulation setup and hyperparameters.

$\|\mathbf{z}_*\|^2/(2\alpha\ell_{RQ}^2))^{-\alpha}$. Their hyperparameters $\gamma_{RBF}, \gamma_{Mat}, \gamma_{RQ}$ and $\ell_{RBF}, \ell_{Mat}, \ell_{RQ}$ denote the kernel scales and length scales, respectively, while ν and α control the Matérn smoothness and the RQ multi-scale behavior. All the relevant hyperparameters are learned via marginal-likelihood maximization as outlined in [2]. In the comparison, we also include the LS and MMSE estimators with full orthogonal training, which serve as the conventional (non-GPR) performance benchmarks.

To evaluate the robustness of the proposed SC-GPR with respect to spatial channel statistics, we consider two channel models for \mathbf{R}_H : the separable Kronecker model [12] and the non-separable Weichselberger model [13]. Under the Kronecker model, the channel covariance is separable across the transmit and receive dimensions, assuming independent spatial correlations at the transmitter and receiver [12]. In contrast, the Weichselberger model yields a generally non-separable covariance matrix \mathbf{R}_H that captures joint transmit-receive coupling through a full power-coupling structure in a common eigenbasis, representing a more general and challenging propagation environment. To assess estimation accuracy, uncertainty calibration, and system-level communication performance, we employ three evaluation metrics, described next.

A. Prediction Error and Posterior 95% Credible Ellipses

We first evaluate the entry-wise complex prediction error $\epsilon_{ij} = H_{ij} - \hat{H}_{ij}$, which is visualized via scatter plots of $\text{Re}(\epsilon_{ij})$ versus $\text{Im}(\epsilon_{ij})$ together with posterior 95% credible ellipses. We compare the proposed SC-GPR method against the RBF, Matérn, and RQ kernel-based GPR baselines from [2] under both the separable Kronecker [12] and the joint-eigenbasis Weichselberger [13] channel models, as shown in Figs. 1a and 1b, respectively. Each scatter plot in Fig. 1 represents the per-entry complex error ϵ_{ij} . Tighter clustering of the scatter points around the origin indicates smaller estimation error, whereas wider dispersion corresponds to higher error variance. Across all pilot subsampling factors $\Delta \in \{2, 3, 4\}$, corresponding to $\{50\%, 67\%, 75\%\}$ pilot savings, it is evident that the proposed SC-GPR consistently achieves the smallest error dispersion among all considered methods. This



(a) Separable covariance structure from Kronecker model.

Fig. 1: Each scatter plot shows $\text{Re}(\epsilon_{ij})$ versus $\text{Im}(\epsilon_{ij})$ per complex channel entry with the empirical posterior 95% credible ellipse; smaller, more isotropic ellipses indicate lower error variance and weaker residual correlation.

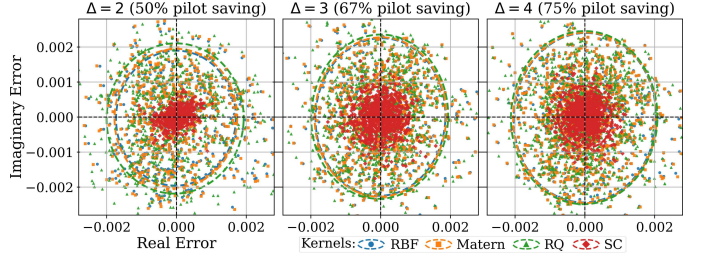
performance gain stems from SC-GPR explicitly encoding the underlying spatial propagation statistics through the \mathbf{R}_H , which generic distance-based kernels are unable to capture accurately, particularly under severe pilot scarcity.

The overlaid 95% credible ellipses characterize the bivariate posterior error distribution. The ellipse area reflects the total error variance, while its orientation and eccentricity capture correlation and anisotropy between the real and imaginary components; larger ellipses therefore indicate higher uncertainty and lower estimation precision. For all reduced-pilot configurations, SC-GPR yields the smallest ellipse areas, confirming superior uncertainty concentration. Moreover, ellipses under the Weichselberger model are generally more isotropic than those under the Kronecker model, owing to the joint-eigenbasis structure of the Weichselberger covariance, which mitigates residual real–imaginary coupling.

B. Uncertainty Calibration (95% coverage)

We assess uncertainty calibration via the empirical coverage of marginal 95% credible intervals for each channel coefficient. For each entry, we compute $\text{Re}(\hat{H}_{ij}) \pm 1.96 \sigma_{ij}^{(\text{Re})}$ and $\text{Im}(\hat{H}_{ij}) \pm 1.96 \sigma_{ij}^{(\text{Im})}$, where $\sigma_{ij}^{(\text{Re})}$ and $\sigma_{ij}^{(\text{Im})}$ are the posterior standard deviations. The empirical coverage is the fraction of true values within these intervals, averaged over the real and imaginary components. For clarity, we only compare against the standard RQ kernel. Table III reports the ellipse area Area_{95} , axis ratio, and empirical coverage probability. The axis ratio, defined as the ratio of major to minor semi-axes of the 95% posterior credible ellipse, is computed from the eigenvalues of the 2×2 covariance matrix of $(\text{Re}(\epsilon_{ij}), \text{Im}(\epsilon_{ij}))$. Values closer to unity indicate more isotropic and weakly correlated uncertainty.

SC-GPR improves coverage relative to baselines and remains reasonably calibrated across all pilot-saving regimes, indicating reliable calibration under reduced training overhead. By contrast, the RQ baseline exhibits similar coverage due to learned lengthscales becoming large relative to the array aperture under sparse sounding, resulting in near-constant correlations and comparable posterior variances. Across both separable and non-separable models, SC-GPR achieves tighter uncertainty concentration and comparable or improved isotropy. These results confirm that SC-GPR provides well-calibrated uncertainty estimates in addition to accurate point estimation. Owing to its greater physical realism, subsequent analyses focus on the Weichselberger model [13].



(b) Joint-eigenbasis covariance structure from Weichselberger model.

| Model | Δ | Error variance (Area ₉₅) | | Axis ratio | | Coverage | |
|----------------|----------|--------------------------------------|-----------|------------|-------|----------|-------|
| | | RQ | SC | RQ | SC | RQ | SC |
| Kronecker | 2 | 1.70e - 5 | 5.93e - 7 | 1.348 | 1.101 | 0.888 | 0.898 |
| | 3 | 2.10e - 5 | 3.13e - 6 | 1.345 | 1.376 | 0.906 | 0.909 |
| | 4 | 2.25e - 5 | 2.41e - 6 | 1.261 | 1.075 | 0.923 | 0.907 |
| Weichselberger | 2 | 1.32e - 5 | 5.86e - 7 | 1.093 | 1.454 | 0.886 | 0.899 |
| | 3 | 1.44e - 5 | 2.23e - 6 | 1.196 | 1.069 | 0.917 | 0.915 |
| | 4 | 1.63e - 5 | 2.16e - 6 | 1.178 | 1.140 | 0.928 | 0.907 |

TABLE III: Posterior 95% credible ellipse metrics comparing baseline RQ and the proposed SC-GPR.

C. Spectral Efficiency

To quantify system-level impact, we evaluate the SE of a multi-stream MIMO link using a linear receiver designed from the estimated channel. For a channel estimate $\hat{\mathbf{H}} \in \mathbb{C}^{N_t \times N_t}$, we adopt the linear MMSE detector $\mathbf{W}(\hat{\mathbf{H}}) = (\hat{\mathbf{H}}\hat{\mathbf{H}}^H + \frac{N_t}{\rho} \mathbf{I}_{N_t})^{-1} \hat{\mathbf{H}} = [\mathbf{w}_1, \dots, \mathbf{w}_{N_t}]$. Let \mathbf{h}_k and \mathbf{w}_k denote the k th columns of the true channel \mathbf{H} and detector $\mathbf{W}(\hat{\mathbf{H}})$, respectively. The post-equalization signal-to-interference-plus-noise ratio (SINR) of stream k is,

$$\text{SINR}_k(\hat{\mathbf{H}}) = \frac{|\mathbf{w}_k^H \mathbf{h}_k|^2}{\sum_{j \neq k} |\mathbf{w}_k^H \mathbf{h}_j|^2 + \frac{N_t}{\rho} \|\mathbf{w}_k\|^2}, \quad (4)$$

where $\hat{\mathbf{H}}$ affects performance only through the detector $\mathbf{W}(\hat{\mathbf{H}})$. The SE is defined as $\text{SE}(\hat{\mathbf{H}}) = \sum_{k=1}^{N_t} \log_2 (1 + \text{SINR}_k(\hat{\mathbf{H}}))$. We evaluate $\text{SE}(\cdot)$ using the true channel \mathbf{H} , the GPR estimate $\hat{\mathbf{H}}_{\text{GPR}}$, and the LS/MMSE baselines $\hat{\mathbf{H}}_{\text{LS}}$ and $\hat{\mathbf{H}}_{\text{MMSE}}$. For LS and MMSE, we use full-array orthogonal training with $T \geq N_t$ and pilot matrix $\mathbf{S} \in \mathbb{C}^{N_t \times T}$. The LS estimate is $\hat{\mathbf{H}}_{\text{LS}} = \mathbf{Y} \mathbf{S}^H (\mathbf{S} \mathbf{S}^H)^{-1}$. Let $\mathbf{y} = \text{vec}(\mathbf{Y})$. The MMSE estimate is $\hat{\mathbf{u}}_{\text{MMSE}} = \mathbf{R}_H \mathbf{A}^H (\mathbf{A} \mathbf{R}_H \mathbf{A}^H + \sigma_n^2 \mathbf{I}_{TN_t})^{-1} \mathbf{y}$ with $\mathbf{A} = \mathbf{S}^T \otimes \mathbf{I}_{N_t}$ and $\hat{\mathbf{H}}_{\text{MMSE}} = \text{unvec}(\hat{\mathbf{u}}_{\text{MMSE}})$, where unvec is the inverse vectorization operator.

Fig. 2 reports the SE achieved by the proposed SC-GPR estimator under pilot subsampling factors $\Delta \in \{2, 3, 4\}$, corresponding to $\{50\%, 67\%, 75\%\}$ pilot savings. Even with 75% pilot savings, SC-GPR consistently outperforms LS across the SNR range. Moreover, for low SNR, SC-GPR with $\Delta \in \{3, 4\}$ achieves higher SE than the full-array training MMSE baseline, while for higher SNR the full-array training MMSE improves and eventually overtakes the reduced-pilot schemes. With 50% pilot savings, SC-GPR closely tracks the true-channel SE and substantially outperforms the full-array training MMSE baseline. This highlights that exploiting

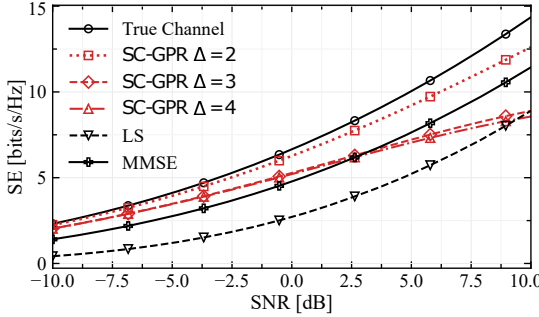


Fig. 2: SE versus SNR comparing the proposed SC-GPR with reduced overheads against ground-truth and LS/MMSE baselines.

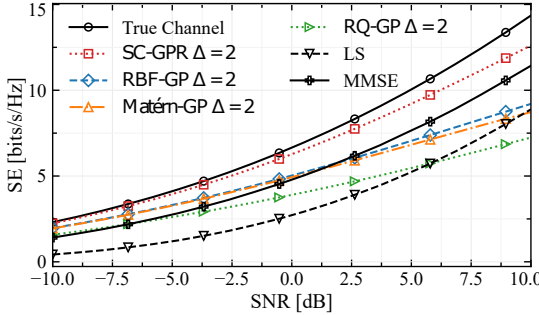


Fig. 3: SE versus SNR comparing SC-GPR with distance-based kernels under 50% pilot savings and LS/MMSE under full pilots.

the spatial covariance structure via the SC kernel can yield superior system-level performance even with reduced training overhead. Fig. 3 compares SC-GPR against learning-based GPR with standard distance-based kernels under 50% pilot savings, while LS and MMSE with 0% pilot savings are included as baselines. SC-GPR most closely matches the true-channel SE, and among the generic kernels the RBF performs best, followed by the Matérn and finally the RQ kernel.

D. Discussion

Table IV summarizes the pilot overhead-performance trade-offs at SNR of 0 dB. The proposed SC-GPR improves estimation fidelity, preserves link-level performance, and reduces training overhead by exploiting \mathbf{R}_H through the SC kernel. It avoids marginal-likelihood hyperparameter optimization and the associated Q -iteration cost, it scales as $\mathcal{O}(P^3)$ with $P = N_r n_t$ rather than $N_r N_t$, and it degrades gracefully as pilot savings increase, whereas learning-based distance kernels are more sensitive to sparse sounding [2]. Consequently, SC-GPR consistently outperforms LS and approaches the full-array training MMSE benchmark with substantially lower training overhead and computational burden.

V. CONCLUSIONS

We proposed a GPR channel estimation framework based on a second-order-statistics-aware SC kernel constructed directly from the channel second-order statistics. The resulting estimator admits a closed-form posterior mean and covariance, eliminates marginal-likelihood hyperparameter learning, and enables uncertainty-aware inference via credible regions. We established that the SC kernel is PSD and showed that

| Estimator | Δ | T / saving | Relative SE [%] | NMSE [dB] | Complexity |
|-----------|----------|---------------------|-----------------|-----------|-------------------------------|
| SC-GPR | 2 | 18 / 50% | 94.5 | -14.75 | $\mathcal{O}(648^3)$ |
| SC-GPR | 3 | 12 / 67% | 80.0 | -9.65 | $\mathcal{O}(432^3)$ |
| SC-GPR | 4 | 9 / 75% | 79.0 | -8.53 | $\mathcal{O}(324^3)$ |
| RBF-GPR | 2 | 18 / 50% | 76.1 | -2.81 | $\mathcal{O}(Q \times 648^3)$ |
| RBF-GPR | 3 | 12 / 67% | 61.3 | -1.67 | $\mathcal{O}(Q \times 432^3)$ |
| RBF-GPR | 4 | 9 / 75% | 46.3 | -1.18 | $\mathcal{O}(Q \times 324^3)$ |
| LS | - | 36 / 0% | 49.5 | -4.96 | $\mathcal{O}(36^3)$ |
| MMSE | - | 36 / 0% | 73.90 | -10.49 | $\mathcal{O}(1296^3)$ |

TABLE IV: Comparison of the proposed SC-GPR with RBF-GPR, LS, and MMSE in terms of pilot overhead, relative SE, NMSE, and computational complexity at 0 dB.

the resulting posterior mean coincides with the corresponding MMSE estimator under the same second-order statistics, without requiring Gaussian channel distributions. Numerical results under both separable and non-separable correlation models demonstrated that SC-GPR achieves substantially lower NMSE and better preservation of spectral efficiency under aggressive pilot reduction, while maintaining lower computational cost than learning-based GPR and full-array training MMSE baselines. Future work will address robustness under covariance mismatch and the extension to time-varying channels.

REFERENCES

- [1] J. Zhu *et al.*, “Electromagnetic information theory-based statistical channel model for improved channel estimation,” *IEEE Trans. Inf. Theory*, vol. 71, no. 3, pp. 1777–1793, 2025.
- [2] S. L. Shah *et al.*, “Low-overhead CSI prediction via Gaussian process regression,” *IEEE Wireless Commun. Lett.*, vol. 15, pp. 1075–1079, 2026.
- [3] N. Rajatheva *et al.*, “White paper on broadband connectivity in 6G,” *6G Research Visions*, no. 10, 2020. [Online]. Available: <https://urn.fi/URN:ISBN:9789526226798>
- [4] S. L. Shah *et al.*, “A novel geometry-aware GPR-based energy-efficient and low-overhead channel estimation scheme,” *arXiv preprint*, 2025. [Online]. Available: <https://arxiv.org/abs/2512.22578>
- [5] Z. Chen *et al.*, “Efficient spatial channel estimation in extremely large antenna array communication systems: A subspace approximated matrix completion approach,” *IEEE Open J. Commun. Soc.*, vol. 6, pp. 1216–1230, 2025.
- [6] E. Vlachos *et al.*, “Massive MIMO channel estimation for millimeter wave systems via matrix completion,” *IEEE Signal Process. Lett.*, vol. 25, no. 11, pp. 1675–1679, 2018.
- [7] C. K. Williams *et al.*, *Gaussian processes for machine learning*. MIT press Cambridge, MA, 2006, vol. 2, no. 3.
- [8] S. L. Shah *et al.*, “Interference prediction using Gaussian process regression and management framework for critical services in local 6G networks,” in *Proc. IEEE Wireless Commun. and Netw. Conf. (WCNC)*, 2025.
- [9] A. Arjas *et al.*, “Nonlinear sparse Bayesian learning methods with application to massive MIMO channel estimation with hardware impairments,” *arXiv preprint*, 2025. [Online]. Available: <https://arxiv.org/abs/2506.03775>
- [10] J. Li *et al.*, “Spatio-temporal electromagnetic kernel learning for channel prediction,” *IEEE Trans. on Wireless Commun.*, vol. 25, pp. 8114–8130, 2026.
- [11] Ö. T. Demir *et al.*, “Spatial correlation modeling and RS-LS estimation of near-field channels with uniform planar arrays,” in *Proc. IEEE Int. Workshop Signal Process. Adv. in Wireless Commun. (SPAWC)*, 2024.
- [12] J.-P. Kermoal *et al.*, “A stochastic MIMO radio channel model with experimental validation,” *IEEE J. Sel. Areas Commun.*, vol. 20, no. 6, pp. 1211–1226, 2002.
- [13] W. Weichselberger *et al.*, “A stochastic MIMO channel model with joint correlation of both link ends,” *IEEE Trans. Wireless Commun.*, vol. 5, no. 1, pp. 90–100, 2006.